Electronic Supplementary Information

Molecular alignment and nanostructure of 1,4,5,8,9,11-hexaazatriphenylene-hexanitrile (HATCN) thin films on organic surfaces†

Hyo Jung Kim[a]*‡, Jeong-Hwan Lee[b]‡, Ji Whan Kim[a], Sunghun Lee[b], Junhyuk Jang[a], Hyun Hwi Lee[c], and Jang-Joo Kim[a,b]*

[a] *Department of Materials Science and Engineering, and The Center for OLED, Seoul National University, Seoul 151-744 (Republic of Korea). Fax: 82 2 889 8702; Tel: 82 2 880 7893; E-mail: hjkim08@snu.ac.kr , jjkim@snu.ac.kr*

[b] *WCU Hybrid Materials Program, Department of Materials Science and Engineering and The Center for OLED, Seoul National University, Seoul 151-744 (Republic of Korea).*

[c] *Pohang Accelerator Laboratory, POSTECH, Pohang, Gyungbuk 790-784 (Republic of Korea)*

† *Electronic supplementary information (ESI) available.*

‡*Contributed equally to this work.*

S1. Water contact angle on various organic films

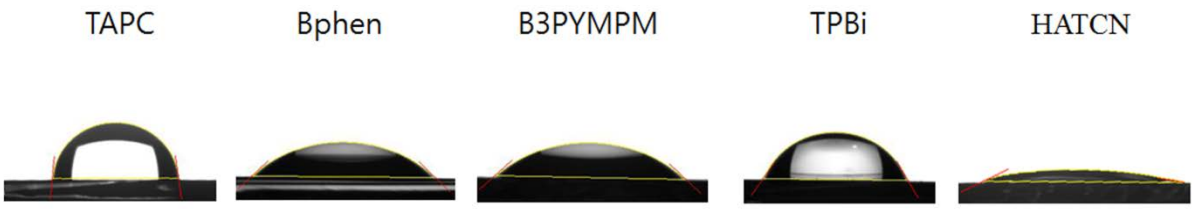

Fig. S1 Distilled water contact angle for TAPC, Bphen, B3PYMPM, TPBi, and HATCN, respectively.

The contact angle of various films was measured using water droplets as shown in figure S1. The contact angle of the TAPC surface shows the highest value of 84° which means TAPC surface is more hydrophobic than the others. However, the contact angle of other ETLs (Bphen, B3PYMPM, and TPBi) were in the range of 43°–56° (Bphen = 44°, B3PYMPM = 43°, and TPBi = 56°). Interestingly, the contact angle of the HATCN surface was almost 0°□ because the HATCN film surface was highly hydrophilic.

S2. Phase image of organic films from AFM measurement

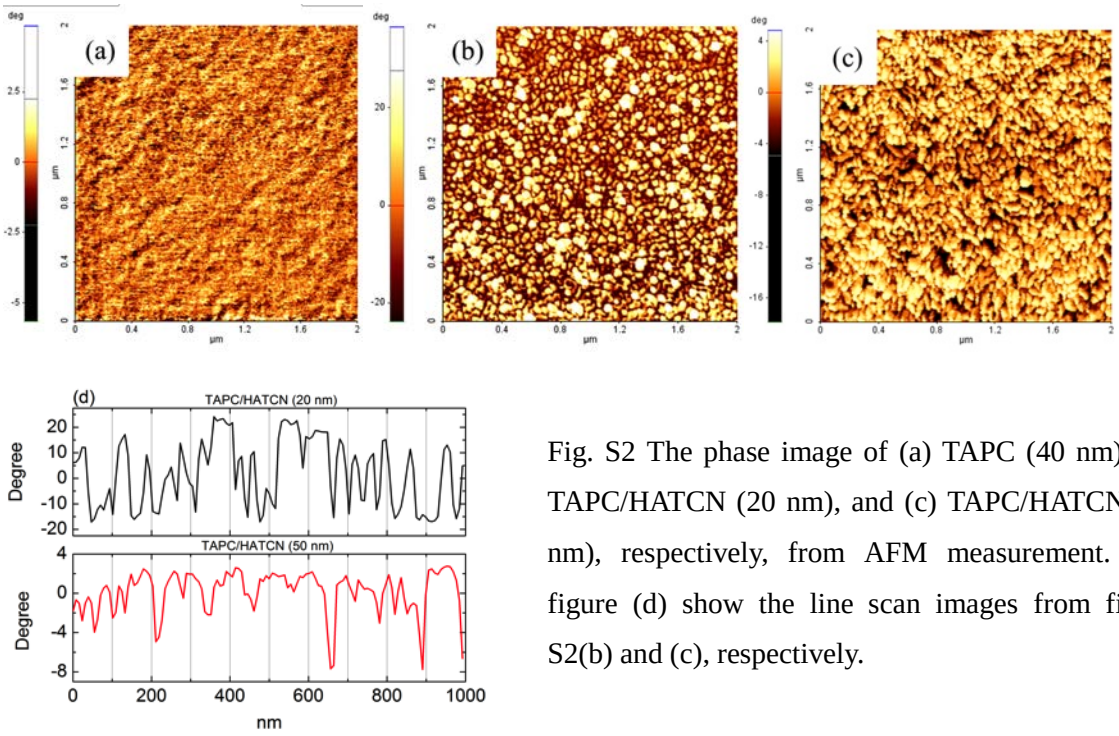

Fig. S2 The phase image of (a) TAPC (40 nm), (b) TAPC/HATCN (20 nm), and (c) TAPC/HATCN (50 nm), respectively, from AFM measurement. The figure (d) show the line scan images from figure S2(b) and (c), respectively.

The Figures show the phase image of the three different films; (a) TAPC (40 nm), (b) TAPC/HATCN (20 nm), and TAPC/HATCN (20 nm). These images show the difference of the grains clearly between the amorphous TAPC film and the discoid HATCN film on it. Moreover, as the thickness of the HATCN film increases from 20 nm to 50 nm, the grain size increases as shown in Fig. S2 (d). In the case of fig. S2(b), more grains are detected in the line scan compared to the case of fig. 2(c). However, we cannot estimate the exact grain size of the film so that we additionally analyse the power spectral density of films, and the results will be discussed in the next page more detail.

S3. Analysis of power spectral density profiles

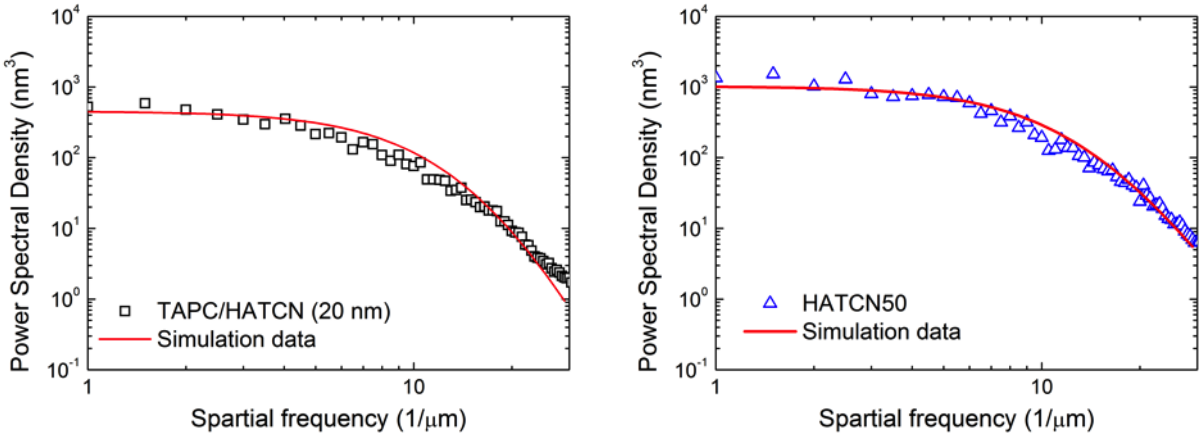

Fig. S3 Open symbols show Power Spectral Density (PSD) profiles of TAPC/HATCN (20 nm) and TAPC/HATCN (50 nm) films, respectively, from AFM measurements. Red line shows the simulation data using ABC model.

The ABC of k-correlation model was used to investigate the grain size of the films quantitatively in the figure 2(c) and (d). The model is defined as follows:[S1]

$$S(f) = \frac{A}{[1 + (B \times f)^2]^{\frac{C}{2}}}$$

Where A is related to the low frequency component of surface roughness, B is related to the grain size and C is the exponent of the power-law fall-of f at high frequencies. The parameters used in the simulation are shown in table 1. The 50 nm-thick-HATCN film showed rough surface and large grain size compared to the 20 nm-thick-HATCN film as listed in the table S1.

Table S1. The three parameters used in the simulation.

	A (nm^2)	B (nm)	C
TAPC/HATCN (20nm)	452	59.1	9.0
TAPC/HATCN (50nm)	1021	68.8	6.5

S4. Crystal size and error values of the HATCN film on the three different ETLs.

Unit [nm]	$(110)_{horizontal}$		$(003)_{vertical}$	
Bphen	28.0	±0.16	10.6	±0.18
TPBi	24.4	±0.26	9.4	±0.11
B3PYMPM	24.2	±0.18	8.6	±0.12

S5. GIWAXS data of 20 nm thick TAPC layer.

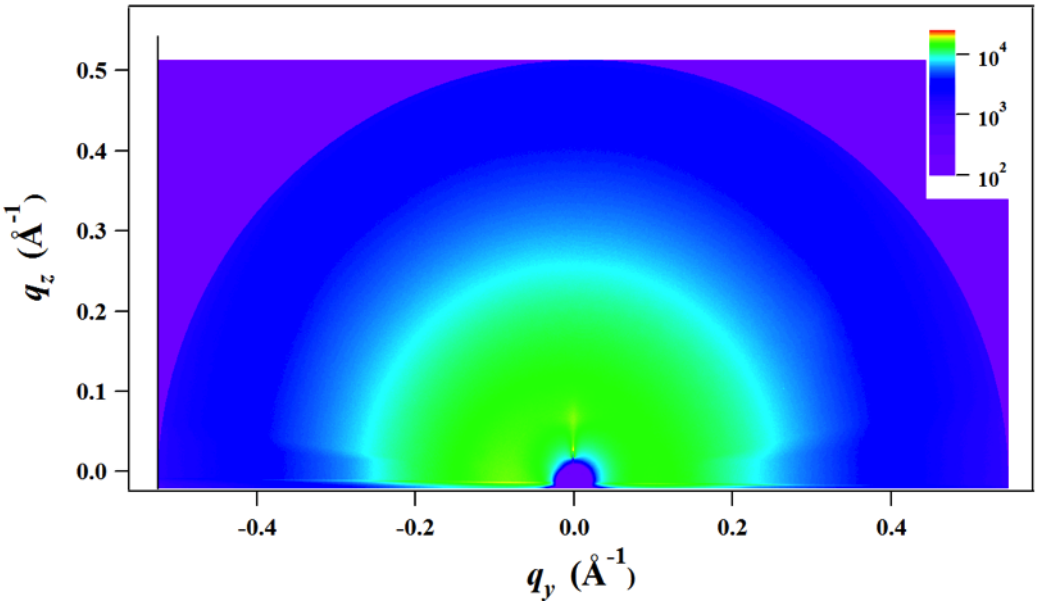

Fig. S5 GIWAXS data of 20 nm thick TAPC layer grown on Si substrate.

References

S1. R. Gavrila, A. Dinescu, D. Mardare, **A power spectral density study of thin films morphology based on AFM profiling**, *Rom. J. Inform. Sci. Technol.* 2007, **10,** 291